Electron paramagnetic resonance and microwave conductivity in pyrolyzed polyacrylonitrile chains included in zeolites

Stéphane Esnouf* and François Beuneu
Laboratoire des Solides Irradiés, École Polytechnique, F-91128 Palaiseau, France

Patricia Enzel† and Thomas Bein
Department of Chemistry, Purdue University, West Lafayette, Indiana 47907

(Received 12 June 1997)

It is possible to polymerize good quality polyacrylonitrile (PAN) chains, typically 360 monomers long, inside the channels of a zeolite. After suitable pyrolysis, these chains become conducting, as proved by microwave measurements and by electron spin resonance. This behavior contrasts with our preceding work with polypyrrole, where the presence of the counterions required for doping very probably blocks the mobility of the charge carriers. In the case of pyrolyzed PAN (PPAN), no such doping is needed, as the carriers appear through the creation of aromatic regions by pyrolysis. The conductivity values obtained prove that the imbedded polymer is a better conductor than the bulk one. Our EPR measurements prove that zeolite-imbedded PPAN undergoes a semiconductor-to-metal transition in the 70–150 K temperature range. Our microwave conductivity measurements imply that this metallic conductivity is restricted to clusters between which the carriers have to jump. [S0163-1829(97)07444-4]

I. INTRODUCTION

The electronic conductivity of various conducting conjugated polymers has been extensively studied for several years. Potential applications of these polymers are numerous: light weight batteries, antistatic equipment, microelectronics, and in a more speculative way molecular electronic devices.

On a more fundamental basis, it would be of great interest to study the properties of such polymer chains when interchain interaction is eliminated or at least reduced. Bein and Enzel[1] have demonstrated the encapsulation of conjugated polymers such as polypyrrole, polyaniline, and polythiophene in the channel system of zeolites. In a previous paper[2] we studied the spin and conductivity properties of encapsulated polypyrrole chains in such zeolites. Our main conclusion was that the ESR signal was due to trapping of polarons and bipolarons by the electrostatic field of the ions present in the periodic zeolite framework, and that this trapping prevented measurable rf and microwave electronic conductivity.

In this context, it seems interesting to study another kind of conducting polymer for which no such ions are needed for doping. Noncharged polymers should give much weaker electrostatic interaction between the conjugated polymer chains and the zeolite channels. One good example of this family of polymers is polyacrylonitrile (PAN) subjected to pyrolysis.[3] Pyrolysis of PAN leads to the formation of a ladder polymer by cyclization through the nitrile pendant group, resulting in two (one C-C and one C-N) conjugated chains. Higher-temperature pyrolysis gives a graphitelike structure, with increasing electrical conductivity.

In this paper we present EPR and microwave conductivity measurements on pyrolyzed PAN (PPAN) chains imbedded in the channel network of two kinds of zeolites (zeolite Y and mordenite). We emphasize here the impossibility of performing dc transport (2- or 4-point) experiments on our samples: the zeolite crystal size is in the micrometer range, thus the included polymer is not accessible to outside contacts; we shall discuss more thoroughly the question of the frequency dependence of conductivity in Sec. V D. A detailed account of the sample preparation and characterization was published elsewhere.[4] This work can be related to the work of Sonobe *et al.* who report the polymerization of PAN in montmorillonite, a two-dimensional matrix.[5]

Literature concerning EPR in PPAN is not always very consistent.[6–9] Hasegawa and Shimizu[7] observe an EPR line with intensity increasing with pyrolysis temperature. Below a pyrolysis temperature of 600 °C, they see a simple signal that they attribute to free radicals. Above 650 °C, they observe two signals, the narrower of which (8–10 G broad) is still attributed to free radicals. The broader signal (30–110 G broad), which decreases with decreasing temperature, is tentatively attributed to conduction electrons. Lerner[8] performs pyrolysis between 435 and 670 °C and sees a single EPR line with some departure from Curie law, which he analyzes in terms of a some Pauli-like contribution to the spin susceptibility. However, he does not see any correlation between the spins and the charge carriers as observed by conductivity measurements. He gives a g-factor value of 2.0028.

Concerning conductivity measurements on pyrolyzed PAN, numerous studies are available,[6,7,10] giving an activated $\exp(-T_0/T)$ law. A hopping mechanism is generally invoked, but little is said about the carriers. We also have to mention Wasserman's measurements on irradiated PAN,[11] giving a $\exp(-T_0/T)^{1/2}$ law.

The present paper deals with experimental details, including sample preparation and characterization and a description of the two experimental techniques (Sec. II): microwave (Sec. III) and EPR (Sec. IV) measurements. Finally we give our present analysis of these results in Sec. V.

TABLE I. The samples. The treatment is done under nitrogen flow (N) or vacuum (*V*).

Sample	Name	*T* of pyrolysis (°C)	Atmosphere	Duration (h)
11	NaY/PPAN	650	*V*	24
12	NaY/PPAN	700	*V*	12
13	NaY/PPAN	700	*V*	24
14	NaY/PPAN	650	N	12
15	NaY/PPAN	650	N	24
16	NaY/PPAN	700	N	12
17	NaY/PPAN	700	N	24
b1	bulk PPAN	600	*V*	12
b2	bulk PPAN	650	N	12

II. EXPERIMENT

A. Sample preparation and characterization

The sample preparation consists of *in situ* polymerization of acrylonitrile in the pores of a zeolite, followed by variable temperature pyrolysis. We used zeolite Y, which is composed of sodalite cages (with 0.3-nm windows) interconnected by double six-rings of Si/Al and of supercages (with 0.8-nm windows) forming a three-dimensional open framework. We summarize here the sample preparation; a more detailed account can be found in Ref. 4. A small amount of degassed zeolite powder (typically 500 mg) is loaded with acrylonitrile vapor for 1 h at room temperature. The amount of monomer loaded is obtained by weighing the sample. The intrazeolite polymerization is then performed in an aqueous solution of potassium peroxodisulfate and sodium bisulfite for 12 h at 40 °C. For the pyrolysis operation, the zeolite/PAN samples are heated in a quartz tube reactor at a rate of 2 °C per min. The target temperature is held for 12 or 24 h; the treatment is done under nitrogen flow or vacuum.

The following characterization was performed: IR spectra, electronic absorption spectra, proton and ^{13}C NMR, gel permeation chromatography, dc conductivity, and thermogravimetric analyses. For some of these experiments, the zeolite network was dissolved with a 25% aqueous solution of HF. The main conclusions are as follows: (i) polymerization does occur in the zeolite framework. (ii) The intrazeolite polymer is very similar to bulk PAN. Chain length analysis reveals a peak molecular weight of about 19 000 (360 monomer units or a length of 0.2 μm, which is roughly the diameter of one individual grain of zeolite) for PAN in zeolite Y and about 1000 (20 monomers) in mordenite. (iii) The zeolite hosts drastically change the pyrolysis reaction. (iv) The zeolite framework is not destroyed during the pyrolysis operation. (v) After recovery from the zeolite hosts, the PPAN shows dc conductivity at the order of 10^{-5} S cm^{-1}.

We give in Table I the main data concerning the zeolite-PPAN samples studied during the present work. The relevant parameters are the pyrolysis temperature (650 or 700 °C), the pyrolysis time (12 or 24 h), and the atmosphere for this pyrolysis (nitrogen or vacuum). While most samples studied for the present work are the zeolite Y samples of Table I, we performed some complementary measurements on some other samples: bulk PPAN, PPAN included in mordenite as host zeolite, and finally PPAN extracted from zeolite Y samples by dissolution of the zeolite matrix.

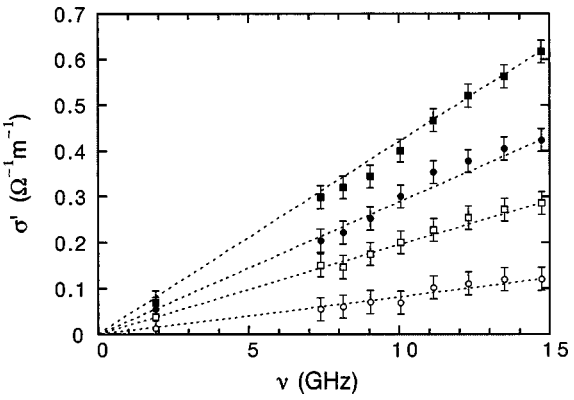

FIG. 1. Microwave conductivity vs frequency for the zeolite Y/PPAN samples at room temperature. Open dots: sample 14; open squares: sample 15; full dots: sample 16; full squares: sample 17.

In order to obtain suitable samples for EPR or microwave conductivity measurements, small amounts of zeolite-PPAN powders (typically 10 mg) were introduced in 4-mm-diameter quartz tubes, which were sealed under an inert atmosphere (He gas).

B. Measurement techniques

EPR spectra are taken using a conventional *X* band Bruker ER200D spectrometer with microcomputer data acquisition. An Oxford Instruments ESR900 liquid helium flow cryostat enables work between 4 and 300 K. Such a cryostat does not enable very reliable temperature measurement, therefore we used a residual Fe^{3+} EPR signal coming from minor iron contamination of the zeolite for temperature calibration, as this signal follows a Curie law.

Microwave conductivity measurements are taken by a cavity perturbation method. The quality factor *Q* of a cavity is measured with an HP8510C network analyzer. For room temperature measurements we use a multimode TE_{10n} rectangular cavity[12] giving 8 resonances with maximum electric field between 7 and 14 GHz. For variable temperature measurements, we use a TM_{010} cylindrical cavity working at 1.9 GHz and cooled by a continuous-flow liquid-helium cryostat. For the two cavities a measurement with an empty tube is required for extracting relevant data as the sample conductivity is proportional to the difference of $1/Q$ with and without sample. The conductivity is deduced from the imaginary part ϵ'' of the dielectric constant epsilon via the formulas $\epsilon''=(V_c/4V_s)\Delta(1/Q)$ (V_c is the cavity volume and V_s the sample volume; an eventual correction from the depolarizing factor can be made here) and $\sigma=\omega\times\epsilon_0\epsilon''$.

III. MICROWAVE CONDUCTIVITY MEASUREMENTS

A. Room temperature measurements

In Fig. 1 we present the variation of the measured conductivity with the microwave frequency, measured at room temperature for the zeolite Y/PPAN samples. Two facts seem to be clear: first, the general tendency is that the conductivity increases with increasing pyrolysis temperature or duration; second, the conductivity increases with increasing

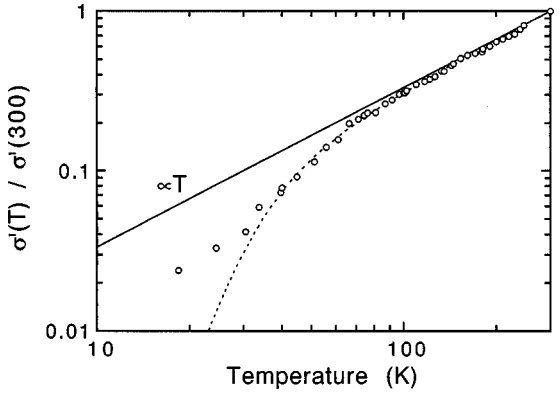

FIG. 2. Microwave conductivity vs temperature at 1.9 GHz for the zeolite Y/PPAN sample 16. The solid line corresponds to a linear fit of the conductivity data for $T>100$ K. The dotted line corresponds to the model given in the text.

frequency; in Fig. 1, the straight lines correspond to a σ proportional to frequency law. Extracted PPAN samples give typically a conductivity 2 or 3 times higher. All samples, however, exhibit a conductivity proportional to microwave frequency in the 2–15-GHz range.

B. Variable temperature measurements

In Fig. 2 we show the variation of the logarithm of the measured microwave conductivity with the inverse temperature, at a frequency of 1.9 GHz, for sample 16. The solid line corresponds to a T law, which is followed above 100 K. We shall discuss this behavior in Sec. V.

IV. EPR MEASUREMENTS

All the samples show a more or less complex EPR signal. A typical spectrum shows a complex line, which can be easily decomposed into two Lorentzian lines. Some other samples exhibit a non-Lorentzian line shape, which again can be computer analyzed as the sum of two Lorentzian lines. These two signals have different behaviors, which we describe now.

A. The narrow signal

The intensity of this signal decreases with increasing pyrolysis time and temperature; no narrow signal can be detected in the samples pyrolyzed at 700 °C. The linewidth ranges from 1.5 to 2 G while the g value is 2.0028. The intensity of the signal follows a Curie law. The number of spins contributing to this signal is small, a typical value being 2.5×10^{15} spins/g (see Table II).

B. The broad signal

In contrast to the preceding one, this signal can be observed in all the pyrolyzed samples, and its intensity increases with the pyrolysis time and temperature. In Fig. 3(a) we give the correlation between the spin magnetic susceptibility (proportional to the number of spins per monomer) corresponding to this broad signal and the microwave conductivity at room temperature as already described. In Fig. 4 we give the variation with temperature of the susceptibility and of the linewidth of a typical signal (sample 13): the temperature law clearly departs from a classical Curie law; the spin susceptibilities given in Fig. 3(a) correspond to the EPR line intensity measured at room temperature. The g factor of this broad line is around 2.003.

V. DISCUSSION

A. Charge carriers and spins

Figure 3(a) shows a clear correlation between the microwave conductivity and the number of spins, both quantities increasing with pyrolysis time and temperature. From this we deduce that pyrolysis induces significant electronic conductivity on the PPAN chains imbedded in the zeolites (of the same order of magnitude as the bulk polymerized polymer), and that the charge carriers involved in this conductivity are also responsible for the broad EPR signal observed.

B. EPR spectra

We attribute the narrow EPR line seen only in samples pyrolyzed at low temperature to intermediate defects during the pyrolysis process, which disappear at higher pyrolysis temperature or time. We will not focus on this signal.

TABLE II. Conductivity and EPR results. χ_{defects}: narrow signal (Sec. IV A); χ_0: broad signal (Sec. IV B), decomposed in two contributions; χ_p: attributed to charge carriers; and χ_c: a Curie-type signal due to localized magnetic moments.

Sample	σ at 8 GHz $(\Omega\ \text{m})^{-1}$	χ_{defects} 10^{15} spins/g	χ_0 10^{-12} emu/g	χ_p 10^{-12} emu/g	χ_c 10^{16} spins/g
11	0.172		3.07	2.40	1.3
12	0.112		2.66	1.41	2.4
13	0.330		8.57	4.34	8.3
14	0.064	2.51	1.89	1.25	1.3
15	0.145	2.33	2.74	2.15	1.2
16	0.192		3.50	2.66	1.6
17	0.269		4.23		
b1	1.6		1500		
b2	1.25		2000		

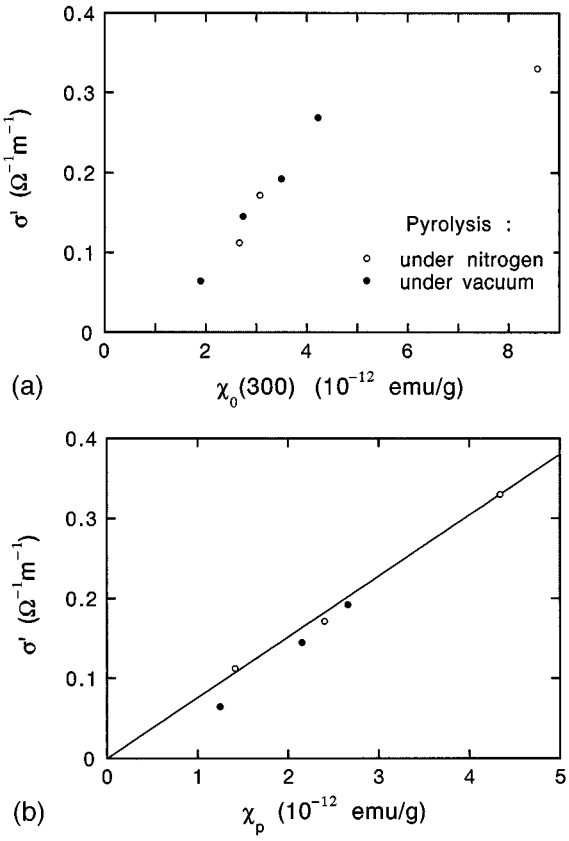

FIG. 3. Correlation, at 300 K, between microwave conductivity (measured at 8 GHz) and spin susceptibility computed from the broad EPR line (a) or spin susceptibility χ_p as analyzed in the text (b). Open symbols represent samples pyrolyzed under vacuum and full ones those pyrolzed under nitrogen.

The variation of spin susceptibility with temperature given in Fig. 4 looks like what is observed in several molecular crystals based on aromatic molecules, such as anthracene[13] and perylene[14]: for these crystals, susceptibility follows a Curie law at low temperature, and then increases exponentially above 50 or 100 K. Such a behavior is interpreted[15] as follows:

(i) The Curie law, which dominates below 100 K, is attributed to some crystal defects giving rise to localized magnetic moments.

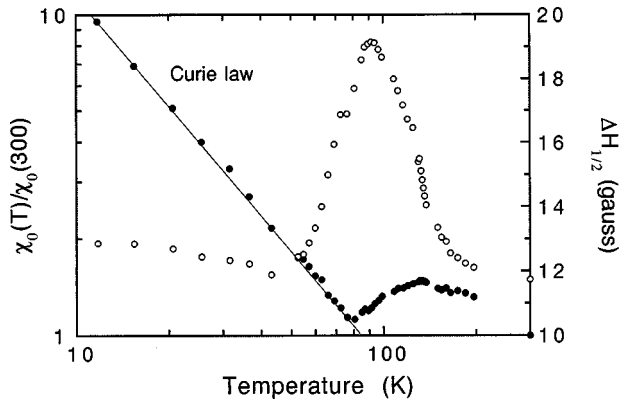

FIG. 4. Variation of the logarithm of the spin susceptibility (full dots) and of EPR linewidth (white dots) vs temperature for sample 13.

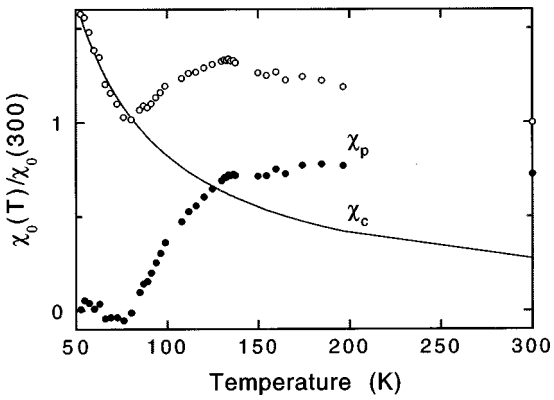

FIG. 5. Variation of spin susceptibility (white dots) vs temperature for sample 13. The line corresponds to the Curie law fit of the low-temperature behavior, whereas the full dots display the χ_p part of the susceptibility.

(ii) For $100<T<150$ K, the rapid broadening of the EPR width indicates a phase transition.

(iii) Above 150 K, the susceptibility increases rapidly and the linewidth becomes constant. In the same T range, conductivity shows a continuous transition from semiconductor to metallic behavior.

For our measurements in PPAN, we see (Fig. 4) that the Curie law is followed under 100 K. For higher temperatures, there is an additional component as shown in Fig. 5, where the full dots correspond to this component, χ_p, after subtraction of the Curie contribution. χ_p is zero below 75 K, rapidly increases above this temperature, and reaches a constant value above 150 K. In this last T region, the behavior of χ_p suggests metallic Pauli behavior. In Fig. 3(b), we replot the data of Fig. 3(a), using χ_p as the new value for the susceptibility: we get now a true proportionality between conductivity and spin susceptibility. We deduce from this that total susceptibility is made up of two contributions: the first from charge carriers and the second from isolated magnetic moments, attributed to localized defects. It is worth mentioning that this last contribution corresponds to $10^{17}-10^{18}$ spins per gram of organic matter, which is much lower than what is observed in bulk PPAN: the structure of the embedded polymer is more ordered than that of the bulk polymer.

We also have to remark that, neglecting the narrow signal described in Sec. IV A, only one line is observed in the whole T range, while the present analysis supposes two distinct contributions. This implies an interaction between the two spin systems, probably through the diffusion of the mobile charge carriers. The rapid variation of the total susceptibility around 100 K can be attributed to a semiconductor to metal transition,[15] and is correlated to the substantial broadening of the line in this T range.

C. Conductivity values

It is interesting to mention here the high conductivity values measured in the present work: see, for instance, the data in Fig. 1. These data can be compared to our measurements on bulk PPAN samples, giving values between 1 and $2(\Omega\ \mathrm{m})^{-1}$ at 8 GHz: these values are not much higher than those for the embedded polymer samples, for which polymer concentration is quite low, of the order of 4 wt %. We con-

clude here that the conducting properties of the embedded polymer are better than those of the bulk polymer. Such behavior is not unexpected, since one may think that embedding reduces disorder and can favor aromatic cluster formation in the supercages or channels of the zeolite host.

D. Variation with frequency and temperature

The microwave conductivity follows with frequency (see Fig. 1) a law in ω^s with s of the order of 1. This is a very common behavior in disordered systems, where there exists a very broad distribution of relaxation times, due to spatial or energetic disorder in the material[16]; in such a case, unfortunately, the frequency dependence of conductivity gives very little information about the physics of transport phenomena.

We analyze now the dependence of conductivity with T, as given in Fig. 2. We model our samples by metallic clusters, as proved by EPR, between which the carriers have to jump through a hopping process to give nonzero conductivity. Such an elementary process is described through a relaxation time τ, with

$$\tau = \tau_0 \exp(U/kT). \tag{1}$$

k is the Boltzmann constant, T the temperature, U an energy barrier to cross, and τ_0 a characteristic time. Such jumps contribute to the conductivity through the following contribution:

$$d\sigma(\omega) = \frac{\ln 2 N e^2 r^2}{3} \frac{i\omega\tau}{1+i\omega\tau}. \tag{2}$$

For the whole system, we consider that there is a distribution of energy barriers to cross, on which a mean has to be taken from the former expression. For high enough frequency, as is the case for our microwave conductivity measurements, one can consider that the carriers perform only a very limited number of jumps during one period of the electric field, so that one can write

$$\sigma(\omega) \propto \left\langle \frac{i\omega\tau}{1+i\omega\tau} \right\rangle. \tag{3}$$

Knowing very little about the barrier distribution, let us consider that the probability $p(U)$ to get a barrier U is constant between two energies U_m and U_M and zero elsewhere. With the assumption that $U_M \gg kT$, we get, for the real part of $\sigma(\omega)$

$$\sigma'(\omega) \propto \frac{\omega kT}{U_M} \left[\frac{\pi}{2} - \arctan(\omega \times \tau_m) \right], \tag{4}$$

where τ_m corresponds to U_m. Assuming, for high enough temperature, that $U_m \ll kT$, we finally get

$$\sigma'(\omega) \propto \frac{\omega kT}{U_M}. \tag{5}$$

Equation (5) is indeed followed above 100 K; see Fig. 2. The departure from linearity obtained below 100 K is quite well described by the dotted line, which is Eq. (4) with $U_m = 8$ meV and $\omega\tau_m = 0.1$. However, this is only a semiquantitative model, as we know from our EPR results that the carrier number is not constant below 100 K.

From our study of the variation of σ with ω and T, we have thus shown that the microwave conductivity in our samples corresponds to disordered systems, where charge carriers follow hopping processes. For our experimental frequencies, conductivity is dominated by jumps between the metallic conducting chains; in order to study intrachain conductivity, one should have to work at frequencies higher than ours, i.e., $\gg 14$ GHz.

VI. CONCLUSION

We have shown that it is possible to polymerize good quality polyacrylonitrile chains inside the channels of a zeolite. After suitable pyrolysis, these chains become conducting, as proved by microwave measurements and by electron spin resonance. This behavior contrasts with our preceding work with polypyrrole, where polymerization was also observed but where no conductivity could be detected. In the case of polypyrrole, the necessity of doping to get charge carriers implies the presence of counterions, which very probably block the mobility of these carriers. In the case of PPAN, no such doping is needed, as the carriers appear through the creation of aromatic regions on the chains by pyrolysis. The conductivity values obtained show that the imbedded polymer is a better conductor than the bulk material. Our EPR measurements prove that zeolite-imbedded PPAN undergoes a semiconductor-to-metal transition in the 70–150-K temperature range. Our microwave conductivity measurements imply that this metallic conductivity is restricted to clusters between which the carriers have to jump.

ACKNOWLEDGMENTS

We acknowledge partial funding for this work by Sprague Electric Co. Fruitful discussions with Professor L. Zuppiroli are greatly appreciated.

*Present address: DSM/DRECAM/SRSIM, Centre d'Études de Saclay, F-91191 Gif sur Yvette, France.

†Present address: Department of Chemistry, Southern Oregon University, Ashland, Oregon 97520.

[1] T. Bein and P. Enzel, Angew. Chem. **28**, 1692 (1989); P. Enzel and T. Bein, J. Chem. Soc. Chem. Commun. **1989**, 1326; P. Enzel and T. Bein, J. Phys. Chem. **93**, 6270 (1989).

[2] L. Zuppiroli, F. Beuneu, J. Mory, P. Enzel, and T. Bein, Synth. Met. **55–57**, 5081 (1993).

[3] A. A. Berlin, J. Polym. Sci. **55**, 621 (1961).

[4] P. Enzel and T. Bein, Chem. Mater. **4**, 819 (1992).

[5] T. Kyotani, N. Sonobe, and A. Tomita, Nature (London) **331**, 331 (1988); N. Sonobe, T. Kyotani, and A. Tomita, Carbon **26**, 573 (1988).

[6] R. M. Valsova and A. V. Airapetyants, Fiz. Tverd. Tela (Leningrad) **7**, 3079 (1965) [Sov. Phys. Solid State **7**, 2488 (1966)].

[7] S. Hasegawa and T. Shimizu, Jpn. J. Appl. Phys. **9**, 958 (1970).

[8] N. R. Lerner, J. Appl. Phys. **52**, 6757 (1981).

[9] A. H. Bhuiyan and S. V. Bhoraskar, Ind. J. Phys. **62A**, 907 (1988).

[10] P. H. Edwig, S. Kulcsar, and L. Kiss, Eur. Polym. J. **4**, 601 (1968); J. L. Jacquemin, A. Ardalan, and G. Bordure, J. Non-Cryst. Solids **28**, 249 (1978).
[11] B. Wasserman, M. S. Dresselhaus, G. Braunstein, G. E. Wnek, and G. Roth, J. Electron. Mater. **14**, 157 (1985); B. Wasserman, Phys. Rev. B **34**, 1926 (1986).
[12] D. C. Dube, M. T. Lanagan, J. H. Kim, and S. J. Jang, J. Appl. Phys. **63**, 2466 (1988).
[13] G. E. Blomgren and J. Kommandeur, J. Chem. Phys. **35**, 1636 (1961).
[14] L. S. Singer and J. Kommandeur, J. Chem. Phys. **34**, 133 (1961).
[15] E. Müller, J. U. von Schütz, and H. C. Wolf, J. Phys. (Paris) Colloq. **3**, 1401 (1986).
[16] J. C. Dyre, J. Appl. Phys. **64**, 2456 (1988).